ACCELERON AEROSPACE JOURNAL (AAJ)
E-ISSN: 2583-9942 (Online) | Accessible at www.acceleron.org.in
Volume 6, Issue 3, (pp.1757-1764)
Article ID: AAJ.11.2106-2612
Research Paper
https://doi.org/10.61359/11.2106-2612

Design and Development of a Morphing-Fin Hybrid Rocket-Powered Loitering Interceptor

Rahul E [*], Ajay Kumar A.M [†], Prof. Madhan Kumar. G [‡]

[1] Bachelor of Aeronautical Engineering, Sathyabama University, Chennai, India – 600119.

[2] Bachelor of Aeronautical Engineering, Sathyabama University, Chennai, India – 600119.

[3] Assistant Professor of Aeronautical Engineering, Sathyabama University, Chennai, India – 600119.

Abstract: The rise of the agile and low-signature aerial threats such as UAVs necessitates the development of advanced and flexible air defence systems. Conventional Surface-to-Air Missiles (SAMs) are often limited by the very low engagement time, while existing loitering munitions are unable to provide the high energy performance needed for intercept. The paper presents the conceptual design and critical analysis of a new type of loitering intercept weapon that combines a throttleable hybrid rocket propulsion system with a mission-adaptive airframe utilizing morphing fins. The methodology for the design consists of the theoretical design of a GOX/HTPB-based hybrid rocket propulsion system capable of high-thrust boost mode (50 N) and low-thrust loiter mode (5 N). The paper also includes the use of Computational Fluid Dynamics (CFD) to assess the aerodynamic performance of the missile in both stowed and deployed fin configurations, validating the aerodynamic feasibility of the low-speed loiter mode. The paper extends the conceptual design by including a critical analysis of the technical challenges.

Table of Contents

1. Introduction

The proliferation of small, agile, and low-cost Unmanned Aerial Vehicles (UAVs) constitutes a major and ever-increasing threat to the air defense infrastructure of today.3 These vehicles have the potential to be used for intelligence, surveillance, and reconnaissance, and/or for direct attack, and they do so in saturating swarms, which make them difficult to counter by conventional means. The motivation for this study stems from the need to create a versatile and cost-effective countermeasure that bridges the performance gap between the conventional high-speed, short-endurance missile and the lower-speed, propeller-driven loitering munition. The present paper introduces an integrated conceptual design for a multi-role interceptor, which leverages the synergistic potential of two cutting-edge technologies, throttleable hybrid-rocket propulsion and morphing aerodynamics, the latter of which has not been explored for SAM applications to date. The objective of this paper is two-fold, namely, to present the conceptual design and preliminary performance assessment of the major subsystems, and to critically analyze the system's architecture and operational concept, the design approach for the propulsion and aerodynamic subsystems, and the system's dynamics and control challenges, and finally, to summarize the major findings and outline the roadmap for the future.

[*]Bachelor of Aeronautical Engineering, Sathyabama University, Chennai, India – 600119. **Corresponding Author:** marshalrahul9@gmail.com.
[†]Bachelor of Aeronautical Engineering, Sathyabama University, Chennai, India – 600119.
[‡]Assistant Professor of Aeronautical Engineering, Sathyabama University, Chennai, India – 600119. **Corresponding Author:** madhan.aero20@gmail.com.
Article History: Received: 17-March-2026 || Revised: 28-March-2026 || Accepted: 28-March-2026 || Published Online: 31-March-2026.

2. System Architecture and Operational Concept

A. System Architecture

The proposed system is a multi-phase interceptor designed for surface- to-air engagements. The architecture integrates a central flight computer with a Guidance, Navigation, and Control (GNC) package, a communications datalink, a payload consisting of an electro- optical/infrared (EO/IR) seeker, a throttleable hybrid rocket motor, and a morphing fin assembly.

B. Concept of Operations (CONOPS)

The CONOPS is envisioned in three distinct phases:

1. **Boost Phase:** Upon launch, the hybrid rocket operates at maximum thrust for rapid acceleration and altitude gain, minimizing the time to reach the operational area.
2. **Loiter Phase:** Once in the designated patrol area, the motor is throttled down to a minimal thrust level. The morphing fins are deployed to maximize the lift-to-drag ratio, enabling the vehicle to patrol efficiently while searching for targets.
3. **Intercept Phase:** Upon target acquisition and designation, the fins are retracted, and the motor is throttled back to maximum thrust for a high-energy terminal intercept, maximizing kinetic energy upon impact.

The sequential flow of the system's operational phases and control logic is illustrated in **Fig 1**.

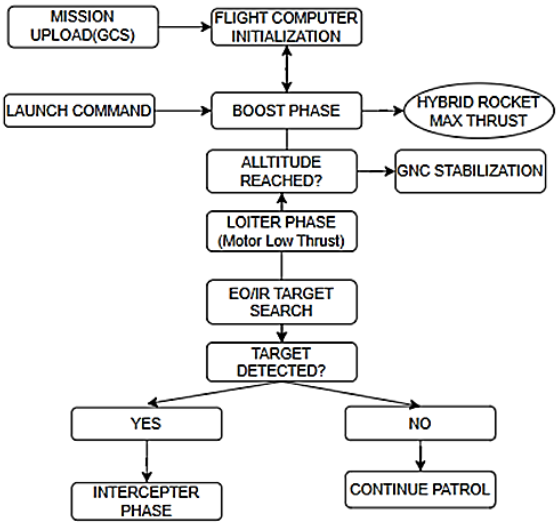

Figure-1. Sequential Flow of the System's Operational Phases

C. Strategic Analysis: A High-Signature Solution for a Low-Signature Problem

A critical evaluation of the proposed CONOPS indicates a limitation in the system architecture, where it is designed to counter small UAVs, which are known to have low acoustic, thermal, and radar signatures. Conventional electric-powered loitering munitions are known to have similar signature characteristics during operation, thereby enabling stealthy surveillance and engagement of targets. However, it is proposed in this system to utilize a hybrid rocket motor, where continuous combustion occurs during operation, thus generating a thermal and acoustic signature. This could potentially compromise stealth during the loitering operation, as it could be easily detected by thermal or acoustic detection systems. Nevertheless, this system also possesses several advantages, such as a high thrust-to-weight ratio, rapid acceleration, and thus enabling quick interception of aerial targets. In this proposed system, stealth is not a priority, and it is focused more on rapid response and interception capability, thereby utilizing high energy propulsion in conjunction with morphing aerodynamic surfaces to ensure efficient loitering in a cost-effective and mechanically simple manner.

Acceleron Aerospace Journal || AAJ.11.2106-2612
Volume 6, Issue 3, pp (1757-1764)
E-ISSN- 2583-9942
https://dx.doi.org/10.61359/11.2106-2612

3. Design and Performance Targets

The propulsion system is a throttleable hybrid rocket motor using Gaseous Oxygen (GOX) as the oxidizer and Hydroxyl-terminated Polybutadiene (HTPB) as the solid fuel. This combination is chosen for its safety, environmental friendliness, and performance characteristics. The fuel regression rate is modelled using the standard empirical power-law relationship :

$$r = aGoxn \qquad Eq(1)$$

The target performance specifications for the motor are summarized in Table 1. These values are considered plausible for a small-scale experimental system, with the specific impulse of 190 s being a realistic, albeit modest, estimate for a GOX/HTPB system accounting for real-world combustion inefficiencies. The external configuration and structural layout of the interceptor are detailed in the 3D CAD models shown in Fig 2 and Fig 3.

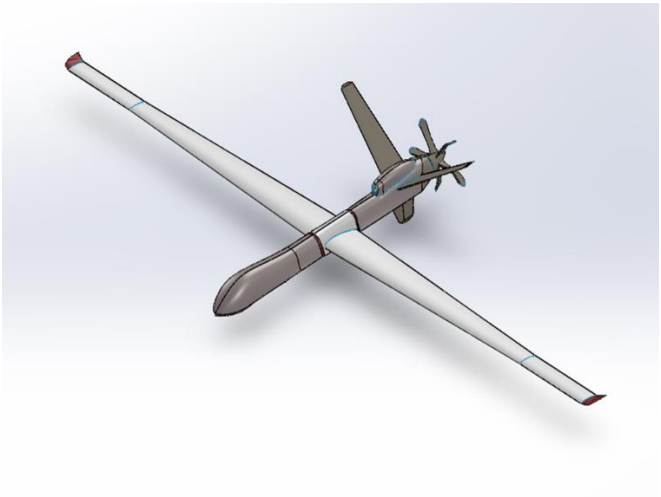

Fig 2: 3d Cad Design with Dimension

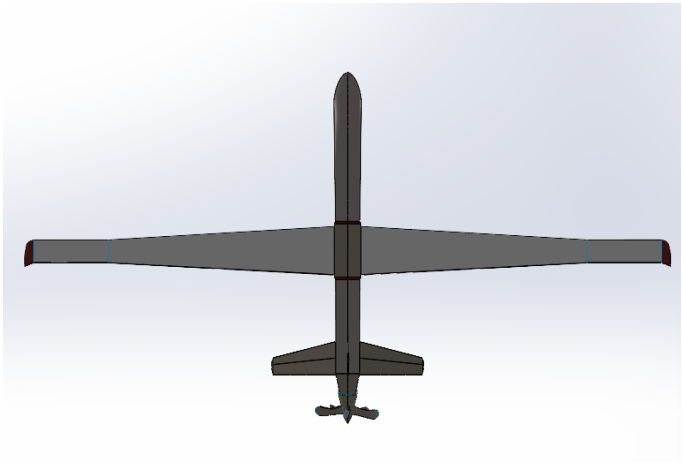

Fig 3: Top View of 3d Cad Design

4. Aerodynamic Design and Analysis

A. Calculation Analysis

The core aerodynamic principle is the use of morphing fins to adapt the airframe for different flight phases. During the low-speed loiter phase, the vehicle must generate sufficient lift to counteract its weight. The required lift coefficient (CL) is given by:

$$CL = \rho \cdot V2 \cdot S2 \cdot m \cdot g0 \qquad Eq(2)$$

This equation shows that at low loiter velocity (V), a very high CL would be required if the vehicle retained its small, low-drag fins (small reference area S). By deploying larger morphing fins, the area S is increased, bringing the required CL down to a practical value achievable at a reasonable angle of attack. CFD analysis confirms this principle, indicating that deploying the fins can significantly increase the lift-to-drag (L/D) ratio, making a sustained loiter phase aerodynamically feasible.

B. Grid Generation:

The mesh refinement strategy, essential for capturing aerodynamic behavior at high speeds, is shown in the tetrahedral grid generation model (As shown in **Fig 4 a & b**).

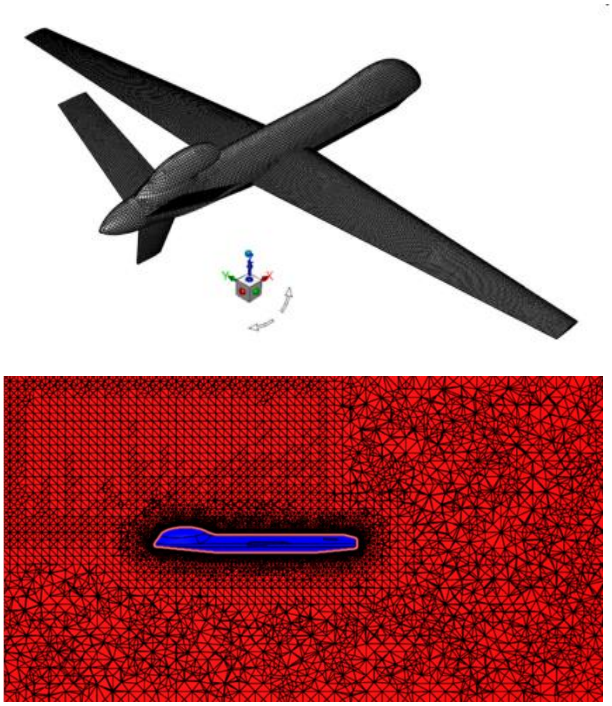

Fig 4: (a)Body Grid (b)Tetrahedral Grid Generation

1) The flow field inlet fluid is air, with an atmospheric density of 0.4135 kg/m3,atmospheric pressure of 26420 Pa, atmospheric temperature of 223 K, speed of sound of 295 m/s, and dynamic viscosity of 1.448 $\times 10^{-5}$ Pa·s at an altitude of 10 km.
2) The flow field inlet is set to pressure far-field with a Mach number of 0.3, and the incoming flow direction is opposite to the aircraft's direction.
3) The flow field outlet is set to outflow.
4) The UAV wing reference area (including the projected area of the wing extending to the fuselage) is 25.754 m2.
5) The UAV's centre of gravity coordinates are set to x = − 6118.339 mm, y = 0 mm, z = 109.146 mm.

The resulting aerodynamic pressure distributions on the UAV body, including static and dynamic pressure nephograms, are presented in **Fig 5.**

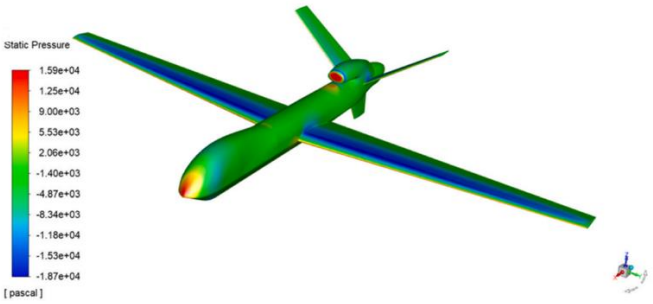

Acceleron Aerospace Journal || AAJ.11.2106-2612
Volume 6, Issue 3, pp (1757-1764)
E-ISSN- 2583-9942
https://dx.doi.org/10.61359/11.2106-2612

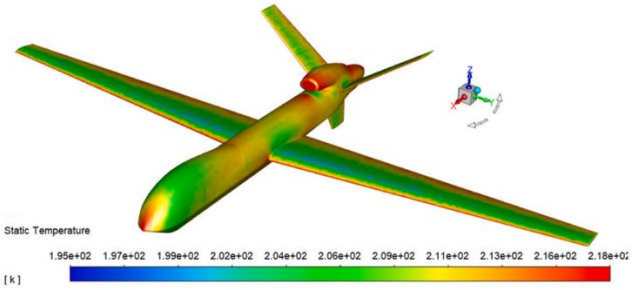

Fig 5: Pressure nephogram of UAV: (a) static pressure, (b) dynamic pressure

C. Calculation on airfoil 0*,10*,20*

The basic geometric relation used in aerodynamics is:

$$\alpha = \tan^{-1}\left(\frac{V_y}{V_x}\right) \quad \text{Eq (3)}$$

Where:

- α= Angle of Attack
- V_x= velocity component along chord line
- V_y= vertical velocity component

The varying airflow characteristics for different angles of attack are visualized in **Fig 6**, with quantitative parameters summarized **in Table 1.**

i. AoA = 0*:

At **0° angle of attack**, the freestream airflow is parallel to the chord line of the airfoil. In this condition, a symmetric airfoil produces nearly zero lift because the pressure distribution on the upper and lower surfaces is nearly identical. However, cambered aerofoils may still produce some lift due to their asymmetric geometry.

Velocity components:

$$V_x = V_\infty$$
$$V_y = 0$$
$$\alpha = \tan^{-1}\left(\frac{0}{V_\infty}\right) = 0^\circ$$

Lift is very small (depending on airfoil camber).

ii. AoA = 10*:

At this AoA, the airfoil produces significant lift and is typically near optimal performance.

At 10° angle of attack, the airfoil is inclined relative to the airflow, causing a higher velocity over the upper surface and lower pressure according to Bernoulli's principle. This creates a significant pressure difference between the upper and lower surfaces, generating lift. In most airfoils, angles around 8°–12° produce efficient lift with moderate drag.

iii. AoA = 20*

At 20° angle of attack, the airfoil experiences a large inclination relative to the airflow. While lift initially increases with increasing AoA, beyond a certain limit known as the stall angle, the airflow begins to separate from the upper surface of the airfoil. This flow separation leads to a sudden reduction in lift and a significant increase in drag. For many conventional airfoils, the stall angle occurs between 15° and 18°, meaning that at 20° AoA the airfoil is typically in a stalled condition.

For 10° angle of attack:

$$V_x = V_\infty \cos\ 10°$$
$$V_y = V_\infty \sin\ 10°$$

Values:

$$\cos\ 10° = 0.9848$$
$$\sin\ 10° = 0.1736$$

Therefore,

$$V_x = 0.9848 V_\infty$$
$$V_y = 0.1736 V_\infty$$

Check AoA:

$$\alpha = \tan^{-1}\left(\frac{0.1736}{0.9848}\right)$$
$$\alpha = 10°$$

$$T = \dot{m} V_e + (P_e - P_a) A_e \qquad \text{Eq(4)}$$

The varying airflow characteristics for different angles of attack are visualized in (As shown in **Fig 6),** with quantitative parameters summarized in **Table 1.**

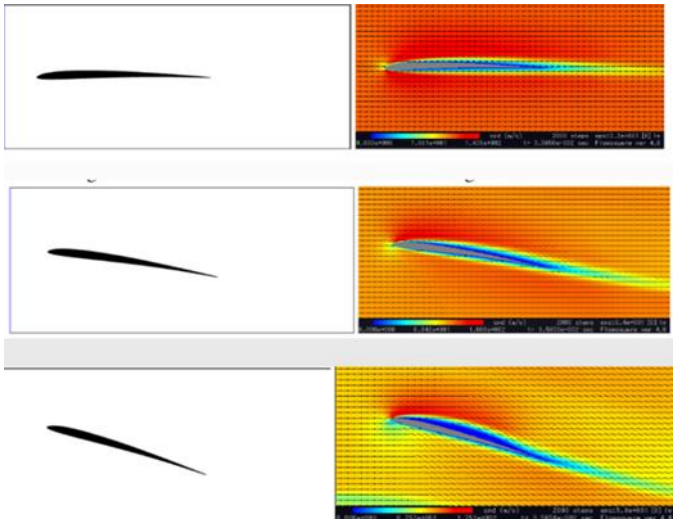

Fig 6: AoA on 0*,10*,20*

Table 1: AoA Parameters

AoA (α)	Vx	Vy	Aerodynamic Behaviour
0*	V infi	0	Minimal lift
10*	0.9848	0.1736	High lift, efficient
20*	0.9397	0.342	Near stall / separated flow

5. Propulsion Efficiency

A GOX/HTPB hybrid rocket propulsion system refers to a hybrid rocket engine that uses Gaseous Oxygen as the oxidizer and Hydroxyl-Terminated Polybutadiene as the solid fuel. In the hybrid rocket propulsion system, the oxidizer is stored under pressure within a tank and then injected into the combustion chamber to burn with the

Acceleron Aerospace Journal || AAJ.11.2106-2612
Volume 6, Issue 3, pp (1757-1764)
E-ISSN- 2583-9942
https://dx.doi.org/10.61359/11.2106-2612

solid HTPB fuel grain to produce high-temperature combustion gases that expand through a convergent-divergent nozzle to produce thru

The internal components of the hybrid rocket motor, including the injector, combustion chamber, and nozzle section, are depicted in the assembly schematic **(As shown in Fig 7).**

Where
T= thrust produced by the rocket
$\dot{m}$= mass flow rate of propellant gases
V_e= exhaust velocity
P_e= exhaust pressure at nozzle exit

P_a= ambient pressure
A_e= nozzle exit area

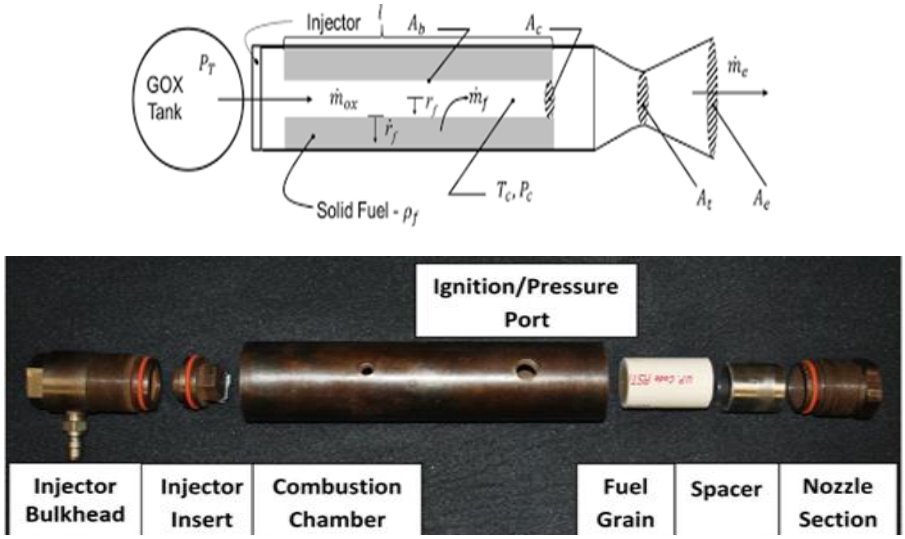

Fig 7: Components of the Combustion Chamber Section

The hybrid rocket motor system has safety advantages over its pure solid and liquid counterparts because its oxidizer is stored separately from the fuel. The solid fuel grain is contained in the combustion chamber, and the oxidizer is contained in an isolated tank. The purpose of the oxidizer feed system is to deliver the oxidizer to the rocket chamber for combustion with the solid fuel grain. A schematic of the oxidizer delivery and power/DAQ systems. The bulk of the system is made up of Swagelok 1/4" stainless steel tubing rated up to 3000 psi and various Swagelok fittings rated up to 5000 psi. Ball valves are installed throughout the system to allow for isolation of any subcomponent. Three manual exhaust valves are installed in-line for pressure relief in the case of a failed solenoid valve or clogged nozzle scenario. Oxidizer and inert gas can be delivered to the combustion chamber during motor firing by remote operation of the solenoid valves. The solenoid valves selected for this assembly are Omega Engineering SV121 high-pressure models which are rated to a maximum pressure of 1450 psi.

6. Conclusion

The specific conclusions of the study are as follows:

[1] When the UAV flies horizontally at Mach 0.3 and 0◦angle of attack in the air of 10 km, its lift coefficient is 0.8888, drag coefficient is 0.0679, the lift-drag ratio is 13.0995, the required thrust is about 2236 N, and the total flying mass of the aircraft is about 3090 Kg.

[2] When the airflow flows through the fuselage, the lift-drag ratio generally shows a wave-like upward trend until it finally stabilizes. The wing tip of the UAV appears turbulence phenomenon, and the closer it is to the airflow of the aircraft fuselage, the lower the velocity is. The positive pressure on the windward side of the UAV is larger, and the temperature is higher than other positions.

[3] Among all the influencing factors analyzed, the angle of attack has the greatest influence on the aerodynamic efficiency of the aircraft, followed by the flying height, and the flying speed has the lowest influence on the aerodynamic performance. In general, it is suggested that the angle of attack should be controlled between 0◦ and 6◦, the flight speed should be controlled near the maximum cruising speed, and the flight altitude should be controlled between 9 km and 11 km.

7. Acknowledgement

The author gratefully acknowledges the support, and expresses deepest gratitude to project supervisor, **Dr. MADHAN KUMAR.G**, for their invaluable guidance, constant encouragement, and critical insights throughout this research. Their mentorship was instrumental in the successful completion of this work. I am also grateful to the Department of Aeronautical Engineering at Sathyabama Institute of Science and Technology for providing the necessary computational facilities and academic environment

8. References

[1] Sutton, G. P., & Biblarz, O. (2016). Rocket propulsion elements (9th ed.). John Wiley & Sons.
[2] Karabeyoglu, M. A., Dyer, J., Stevens, J., & Cantwell, B. (2004). Combustion and thrust-vectoring in a swirling-oxidizer-flow-type hybrid rocket engine. AIAA/ASME/SAE/ASEE Joint Propulsion Conference and Exhibit.
[3] Chiaverini, M. J., & Kuo, K. K. (Eds.). (2007). Fundamentals of hybrid rocket combustion and propulsion. AIAA. https://doi.org/10.2514/4.866876.
[4] Mukunda, H. S., Jain, V. K., & Paul, P. J. (1979). A review of hybrid rockets: Present status and future potential. *Proceedings of the Indian Academy of Sciences Section C: Engineering Sciences*, *2*(2), 215-242. https://doi.org/10.1007/BF02845033.
[5] Barbarino, S., Bilgen, O., Ajaj, R. M., Friswell, M. I., & Inman, D. J. (2011). A review of morphing aircraft. Journal of Intelligent Material Systems and Structures, 22(9), 823-877. https://doi.org/10.1177/1045389X11414084.
[6] Weisshaar, T. A. (2013). Morphing aircraft systems: Historical perspectives and future challenges. Journal of Aircraft, 50(2), 337-353. https://doi.org/10.2514/1.C031456.
[7] Woods, B. K., & Friswell, M. I. (2013). The 'hingeless' morphing wing: A concept for multiple flight modes. Journal of Intelligent Material Systems and Structures.
[8] Zarchan, P. (2012). Tactical and strategic missile guidance (6th ed.). AIAA. https://doi.org/10.2514/4.105845.
[9] Yanushevsky, R. (2007). Modern missile guidance. CRC Press. https://doi.org/10.1201/9781351202954.

9. Conflict of Interest

The author declares no competing conflict of interest.

10. Funding

No funding was issued for this research.